

SUPPLEMENTAL INFORMATION

Tracking Precursor Degradation During the Photo-induced Formation of Amorphous Metal Oxide Films

Kevan E. Dettelbach,^a Danielle A. Salvatore,^b Adam Bottomley,^a Curtis P. Berlinguette^{a,b,c*}

^aDepartment of Chemistry, The University of British Columbia, 2036 Main Mall, Vancouver, BC V6T1Z1.

^bDepartment of Chemical & Biological Engineering, The University of British Columbia, 2360 East Mall, Vancouver, BC V6T1Z3.

^cStewart Blusson Quantum Matter Institute, The University of British Columbia, 2355 East Mall, Vancouver, BC V6T1Z4.

*Correspondence to: cberling@chem.ubc.ca (CPB)

FeO_x-UV-air



FeO_x-NIR-air



FeO_x-UV-N₂



FeO_x-NIR-N₂



Figure S1. Photographs of FeO_x-UV-air, FeO_x-NIR-air, FeO_x-UV-N₂, and FeO_x-NIR-N₂ deposited on FTO. Images were taken against white paper and have been cropped to the edges of the samples.

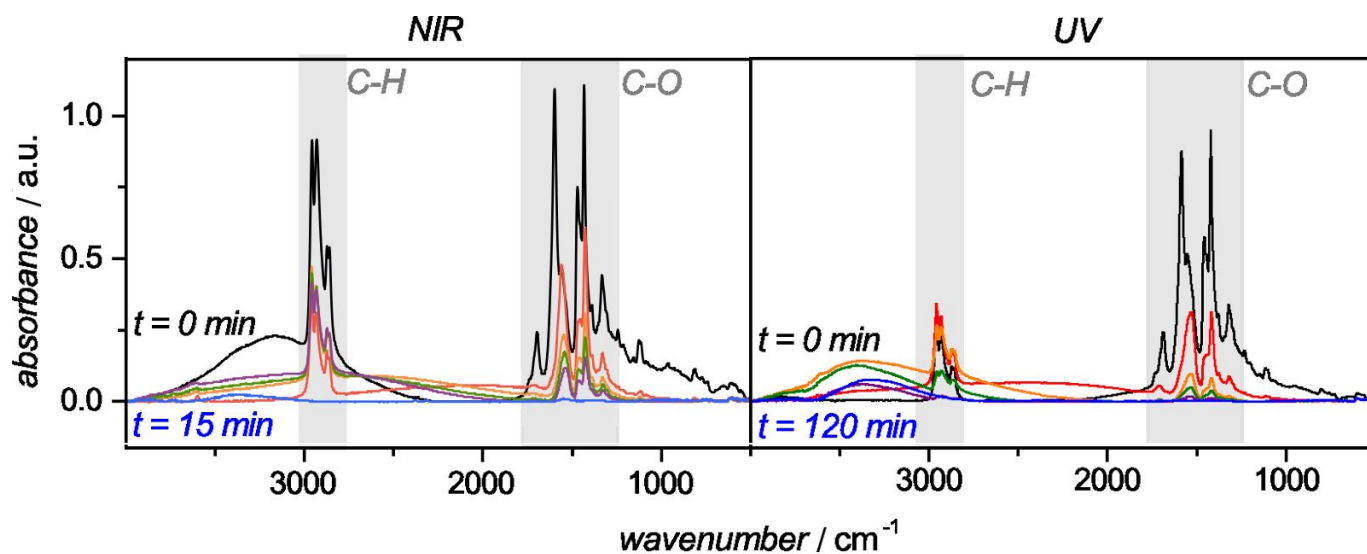


Figure S2. FTIR spectrographs recorded during the NIRDD and UVDD of Fe(eh)₃ performed in air. Data for the formation of FeO_x-NIR-air was recorded at: 5 (red), 7 (orange), 10 (green), 12 (purple) and 15 min (blue). Data for the formation of FeO_x-UV-air was recorded at: 5 (red); 15 (orange); 30 (green); 60 (purple); and 120 min (blue). Both samples showed a diminution of C-H and C-O stretch peaks as a function of time.

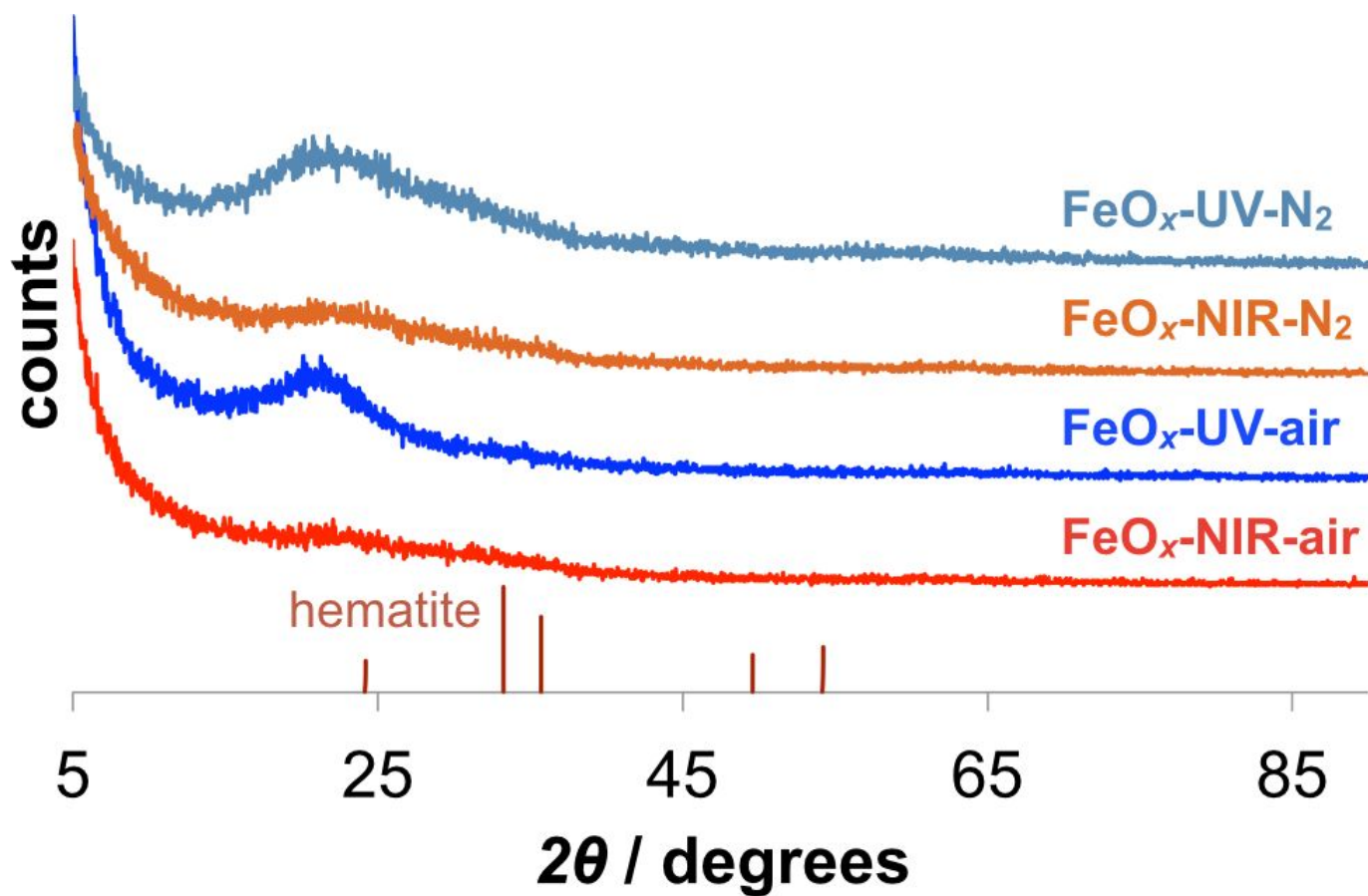


Figure S3. Grazing incidence X-ray diffraction (GIXRD) data recorded for **FeO_x-NIR-air** (red), **FeO_x-UV-air** (blue), **FeO_x-NIR-N₂** (orange), and **FeO_x-UV-N₂** (teal) deposited on glass. Peaks corresponding to crystalline phases of iron oxide were not observed. Hematite is shown for reference (pdf number: 089-8104). The angle of incidence = 0.35°.

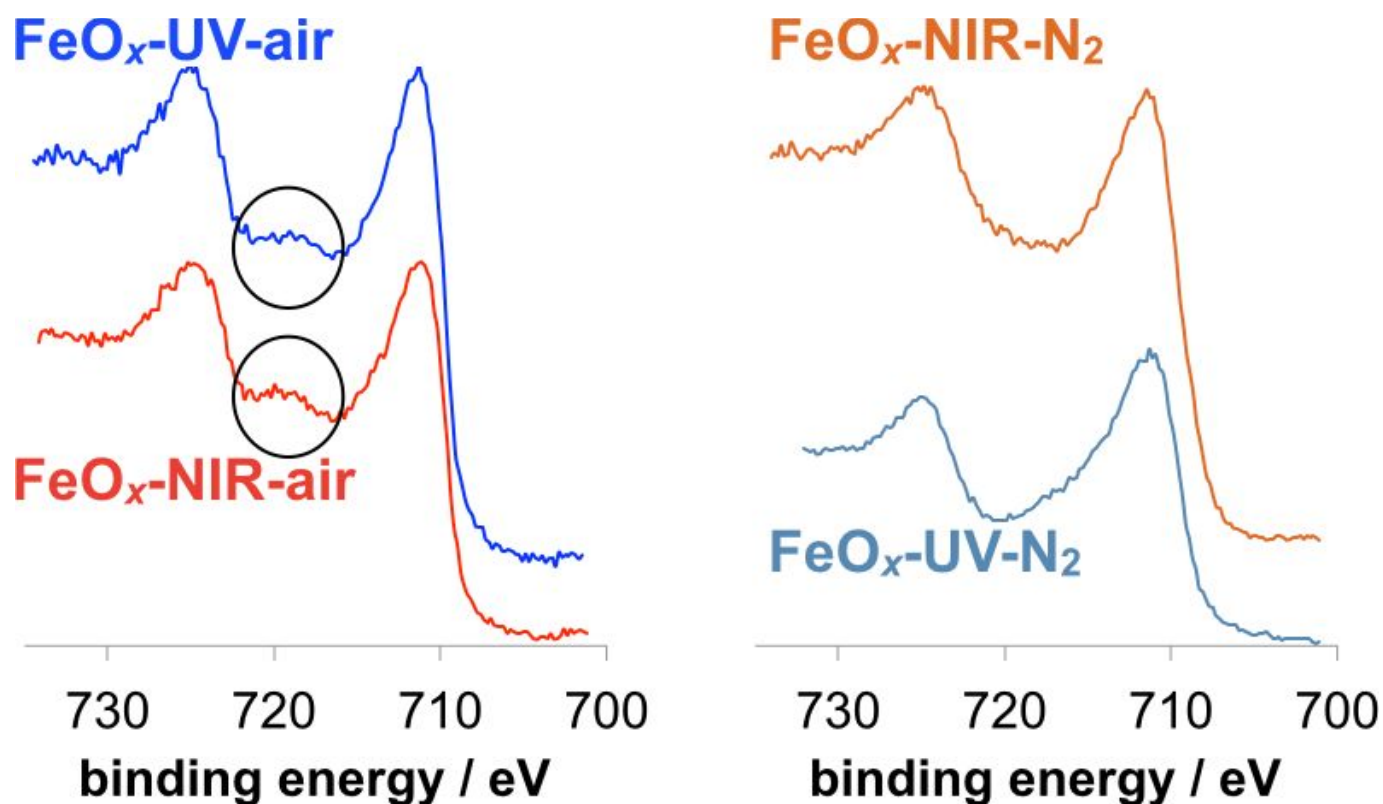


Figure S4. X-ray photoelectron spectra detailing the Fe 2p region for **FeO_x-NIR-air** (red), **FeO_x-UV-air** (blue), **FeO_x-NIR-N₂** (orange), and **FeO_x-UV-N₂** (teal) deposited on glass. The data for both **FeO_x-NIR-air** and **FeO_x-UV-air** displayed Fe(III) satellite peaks (circled in black) consistent with surface ferric sites. The data for **FeO_x-NIR-N₂** and **FeO_x-UV-N₂** lacked observable Fe(III) satellite peaks. These satellite peaks have shifted to higher binding energies and are obscured by the leftmost Fe 2p peak which is an indication that the surface contains both ferrous and ferric sites.¹

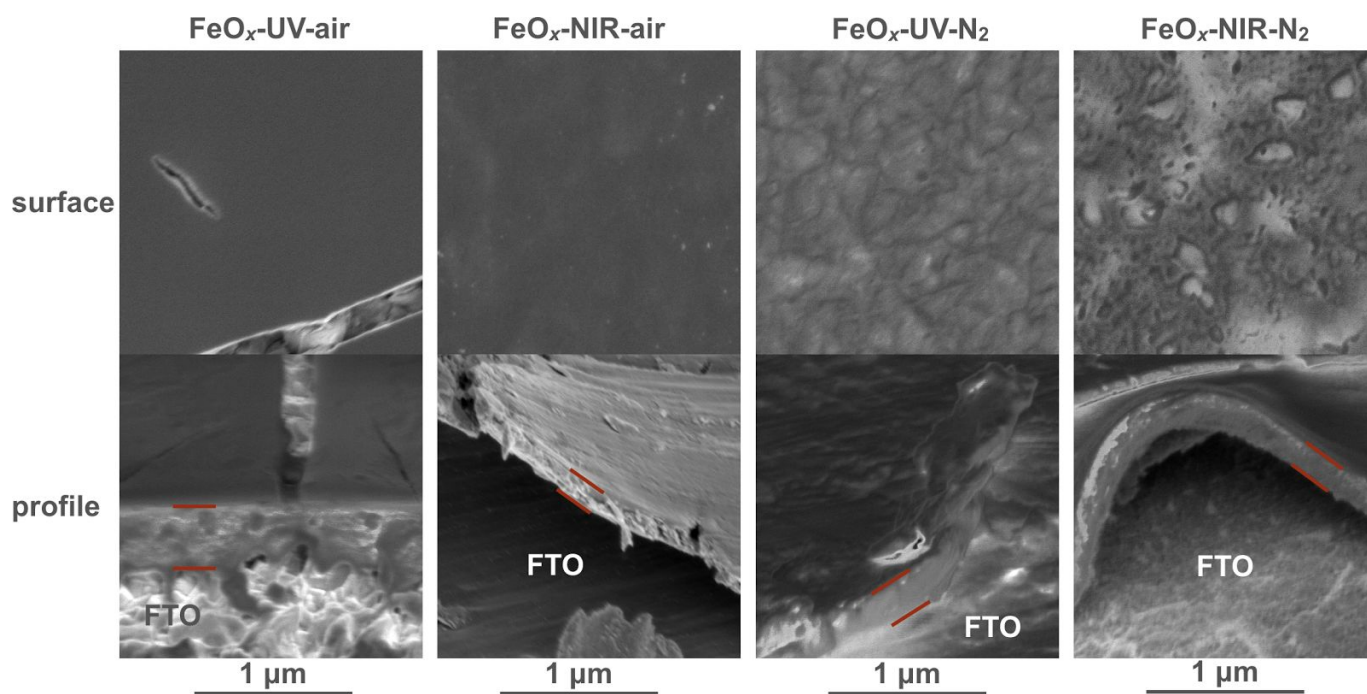


Figure S5. Scanning electron micrographs for FeO_x -UV-air, FeO_x -NIR-air, FeO_x -UV- N_2 , and FeO_x -NIR- N_2 deposited on FTO showing both surface and profile views. The profile of FeO_x -UV-air was made by imaging existing cracks in the film. Profiles of the other samples were made by scratching the sample with a metal stylus and then imaging sections of the film that had detached from the underlying FTO. The red lines indicate the upper and lower edges of the profile. Profiles were imaged at a tilt angle of 52° and the images were corrected for tilt.

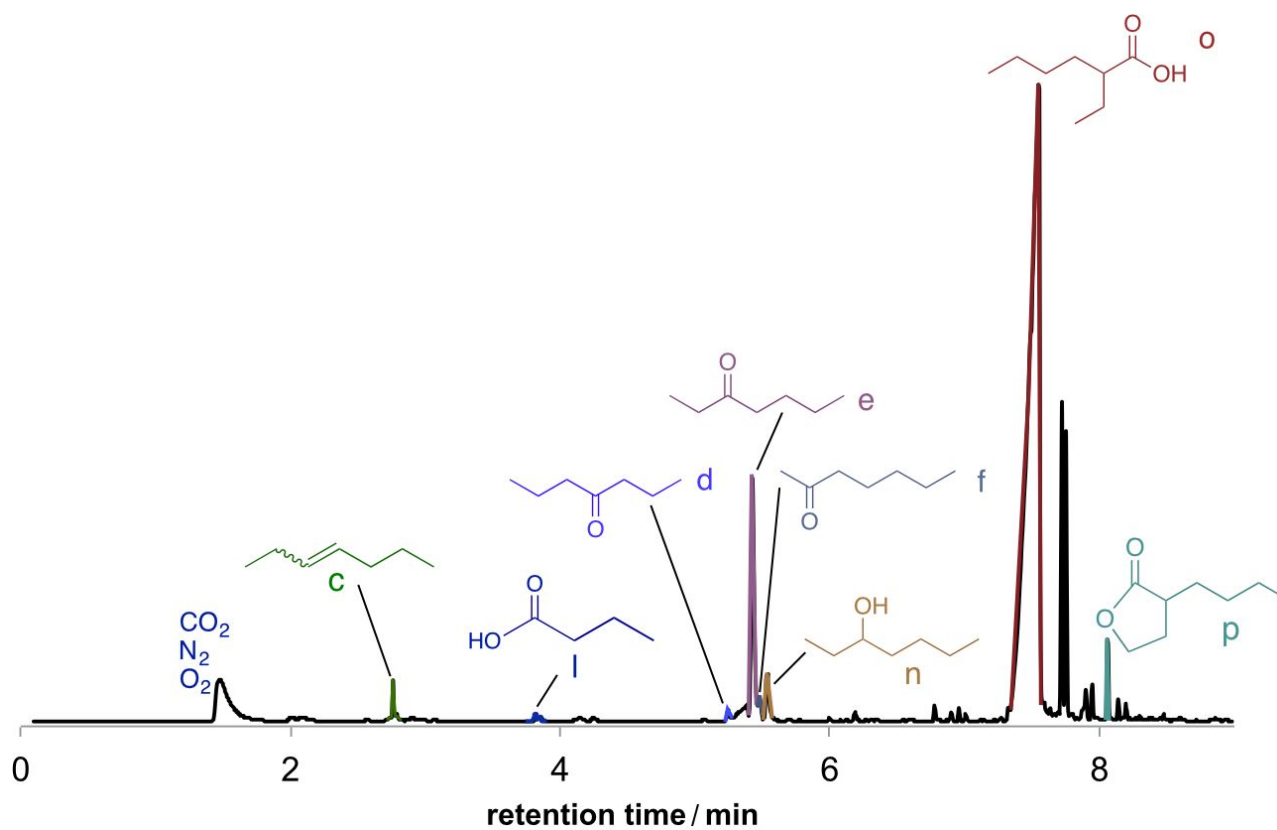


Figure S6. Gas chromatogram trace for the headspace of a sealed cuvette containing $\text{Fe}(\text{eh})_3/\text{FTO}$ heated to 200 °C. This trace is similar to a trace obtained from the headspace of a cuvette containing $\text{Fe}(\text{eh})_3/\text{FTO}$ that was exposed to NIR radiation (Figure 4).

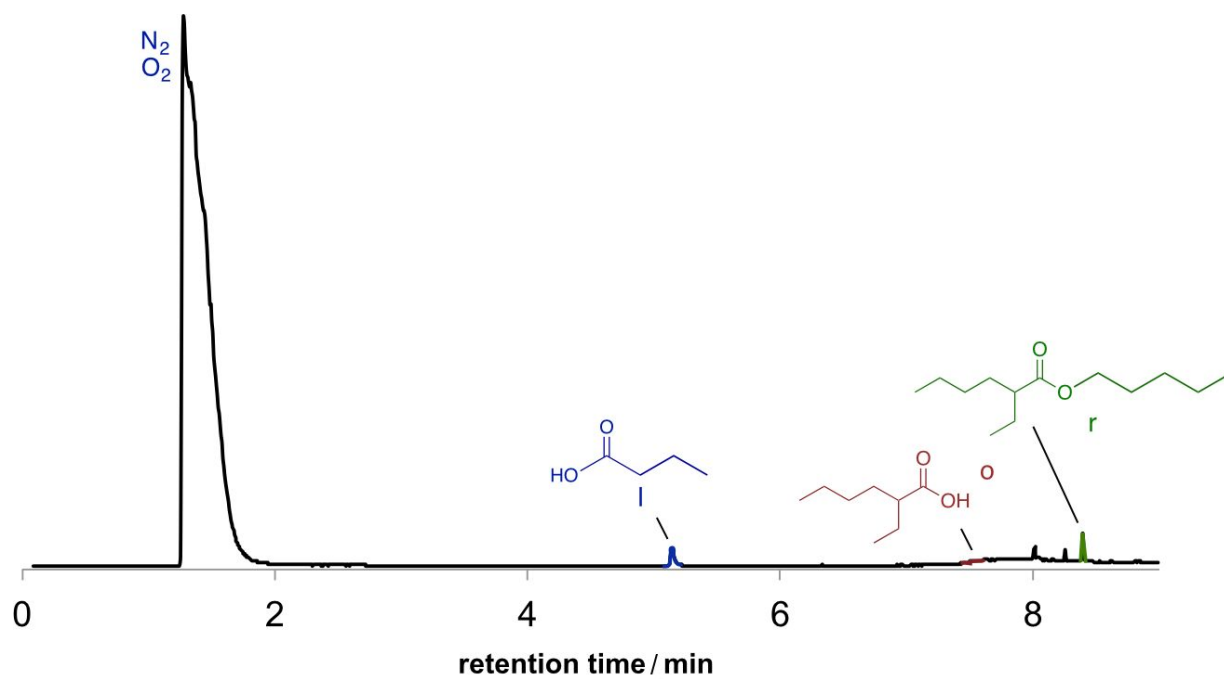


Figure S7. Gas chromatogram traces for the headspace of a sealed cuvette containing $\text{Fe}(\text{eh})_3/\text{FTO}$ heated to 100 °C.

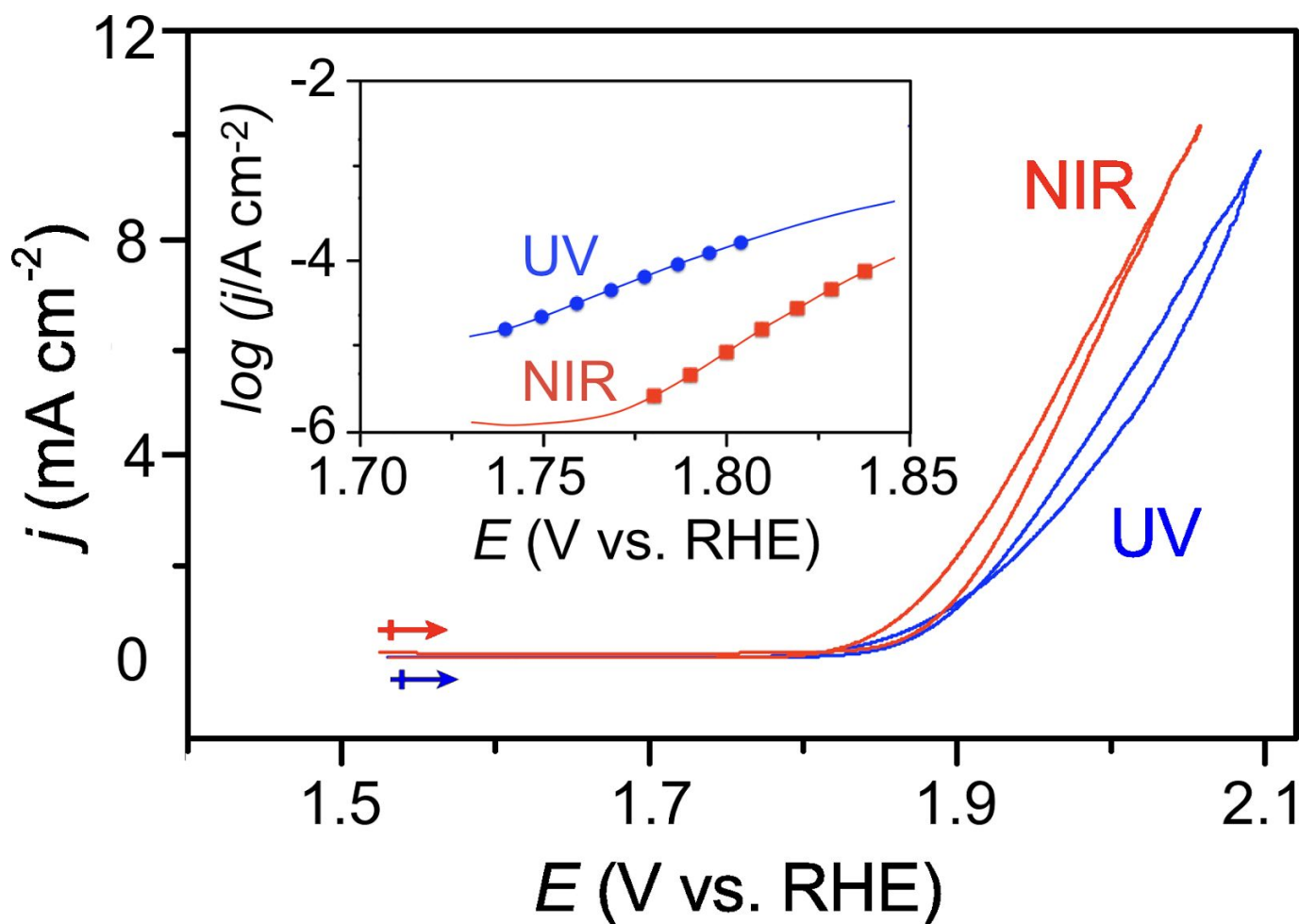
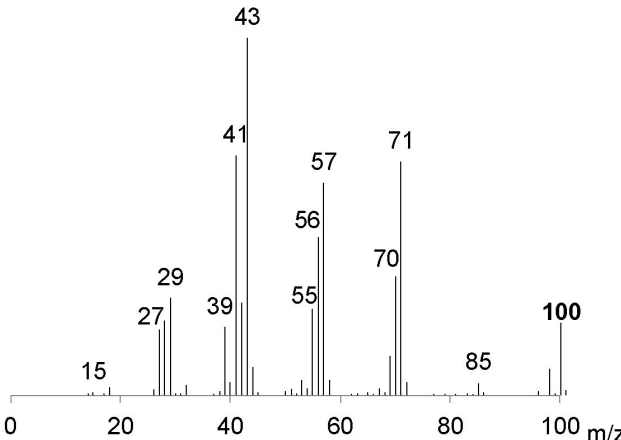
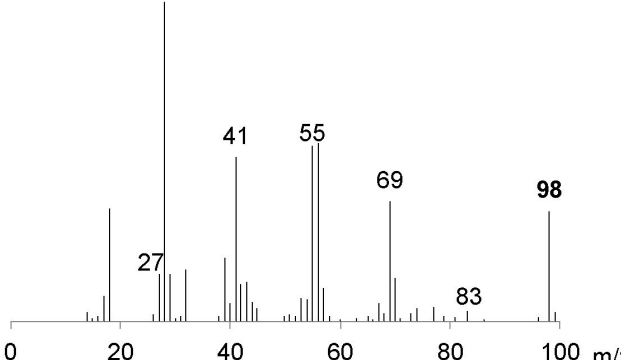
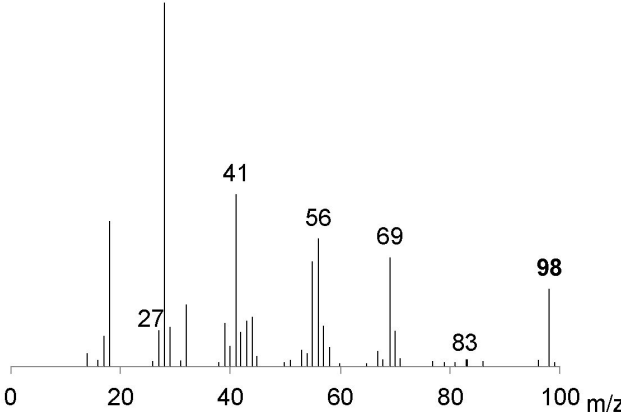
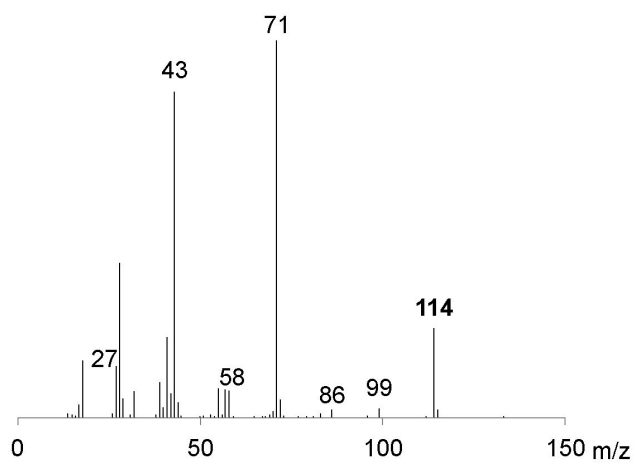


Figure S8. Cyclic voltammograms recorded on FeO_x-UV-N₂ (blue) and FeO_x-NIR-N₂ (red) at a scan rate of 10 mV s⁻¹ in 0.1 M KOH show similar but not superimposable oxidative behavior. Inset: Tafel plots collected by staircase voltammetry (10-mV intervals) show similar onsets of water oxidation ($\eta = 0.51$ V, 0.55 V respectively) but different Tafel slopes (65 mV/dec and 40 mV/dec, respectively).

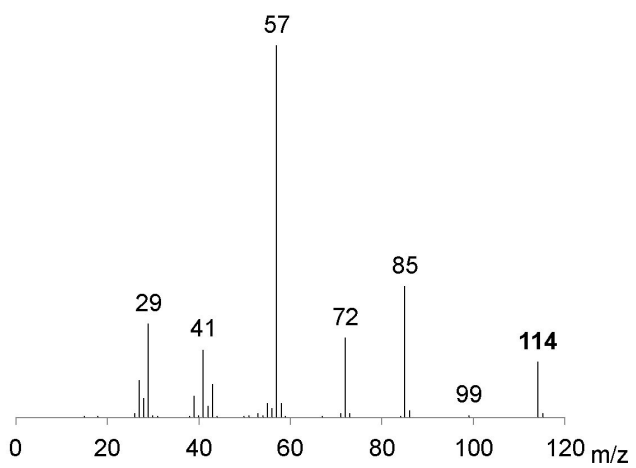
Table S1. Listing of Mass Spectra and the Corresponding Assignments for all Identified Products from the Decomposition of Iron(III) tris-(2-ethylhexanoate) by UV and NIR Light Exposure.

a	product	mass spectrum*
	heptane	 <p>Mass spectrum of heptane showing characteristic peaks. The base peak is at m/z 43. Other significant peaks are labeled at m/z 15, 27, 29, 39, 41, 55, 56, 57, 70, 71, 85, and 100.</p>
b	2-heptene	 <p>Mass spectrum of 2-heptene showing characteristic peaks. The base peak is at m/z 41. Other significant peaks are labeled at m/z 27, 55, 69, 83, and 98.</p>
c	3-heptene	 <p>Mass spectrum of 3-heptene showing characteristic peaks. The base peak is at m/z 41. Other significant peaks are labeled at m/z 27, 56, 69, 83, and 98.</p>

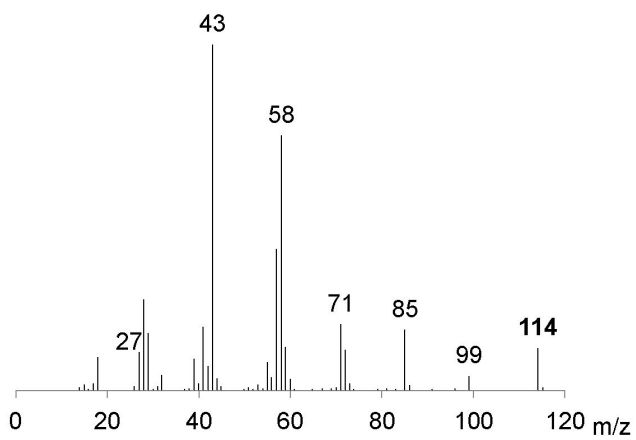
d 4-heptanone



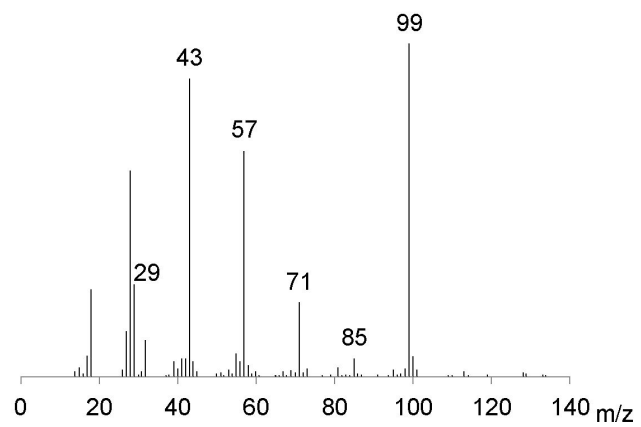
e 3-heptanone



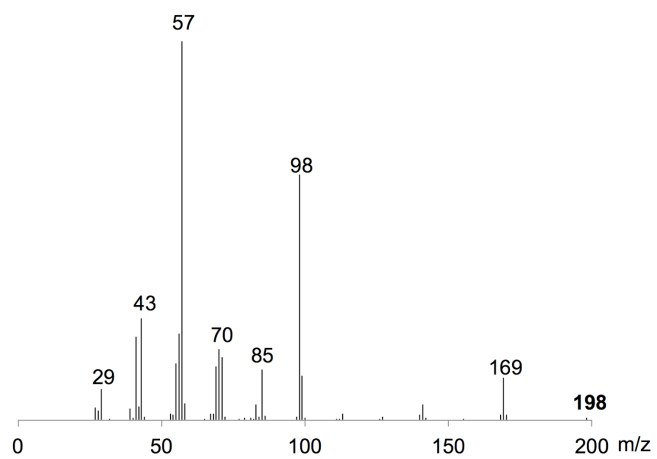
f 2-heptanone



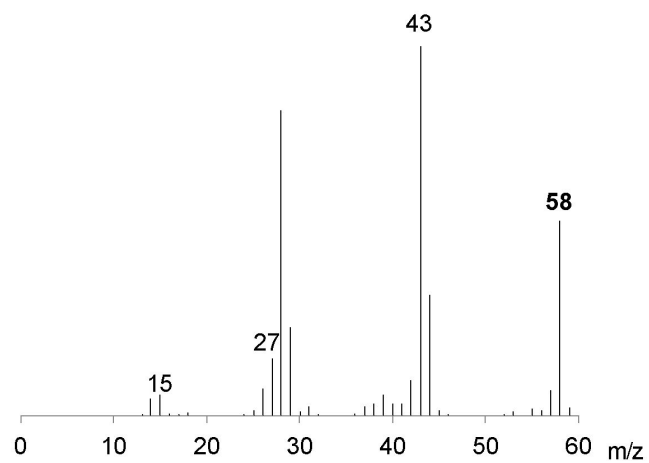
g 3,6-heptanedione



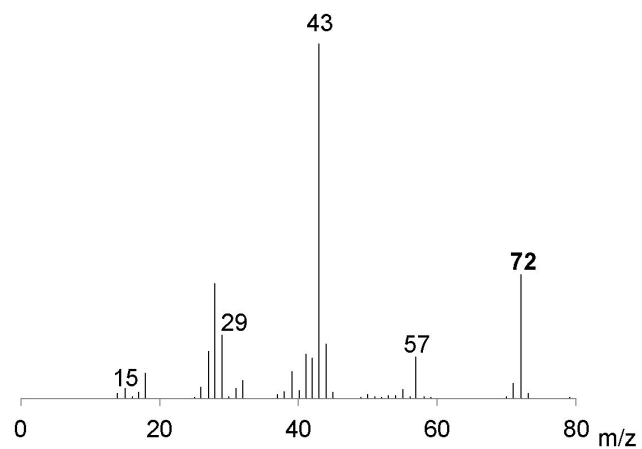
h 5,6-diethyldecane



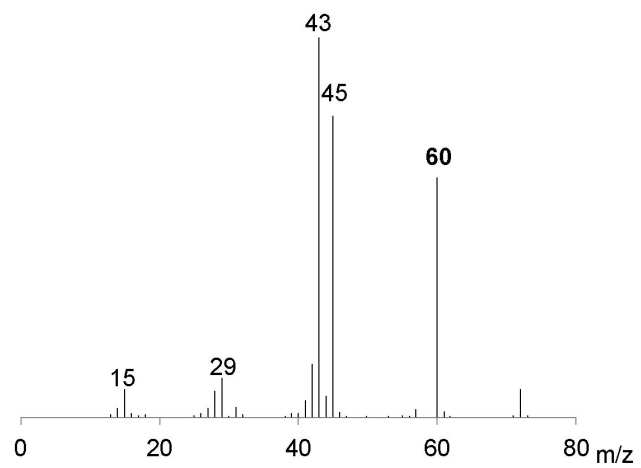
i acetone



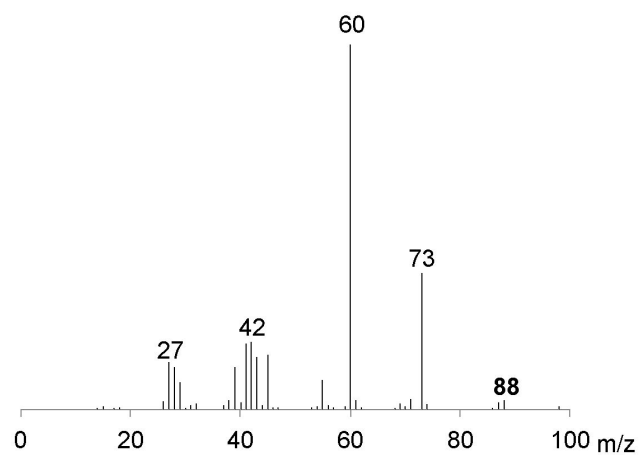
j butanone



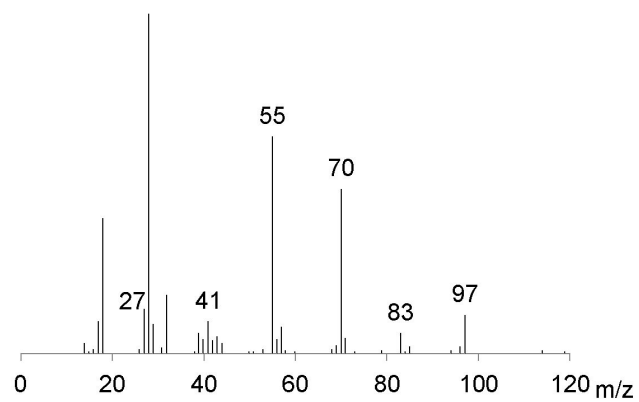
k acetic acid



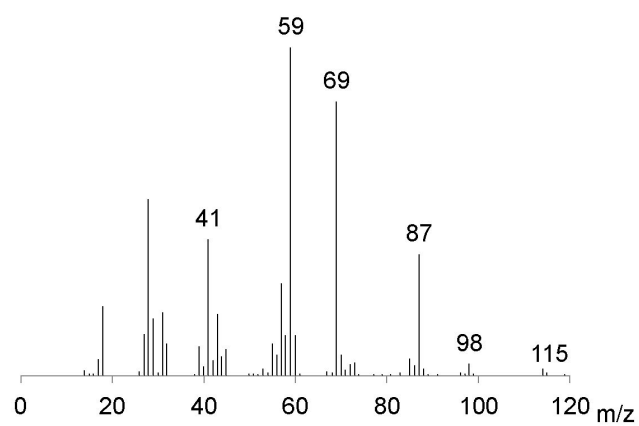
l butanoic acid



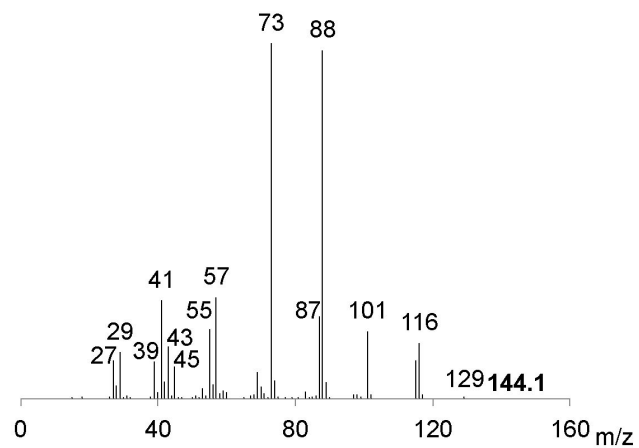
m 1-hepten-3-one



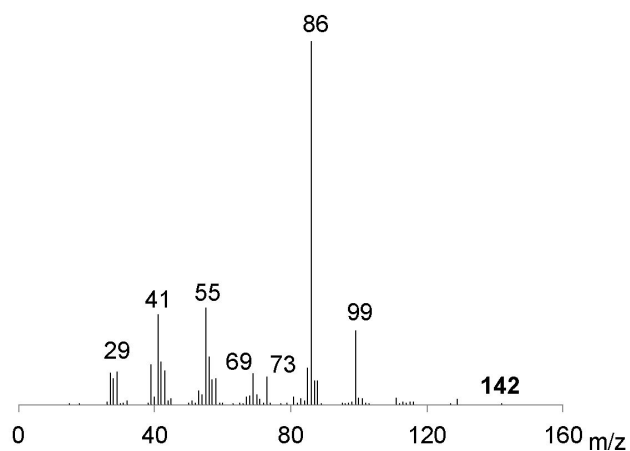
n 3-heptanol



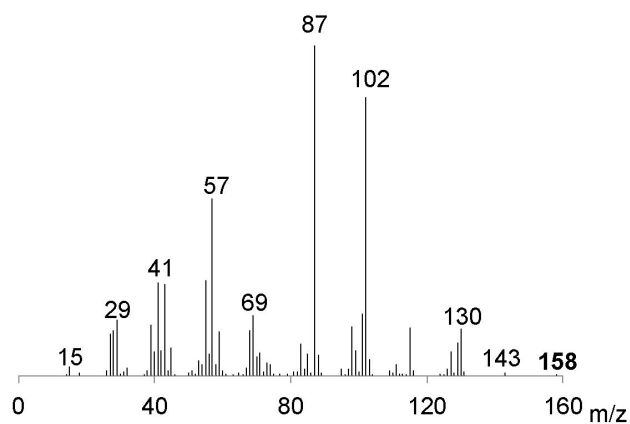
o 2-ethylhexanoic acid



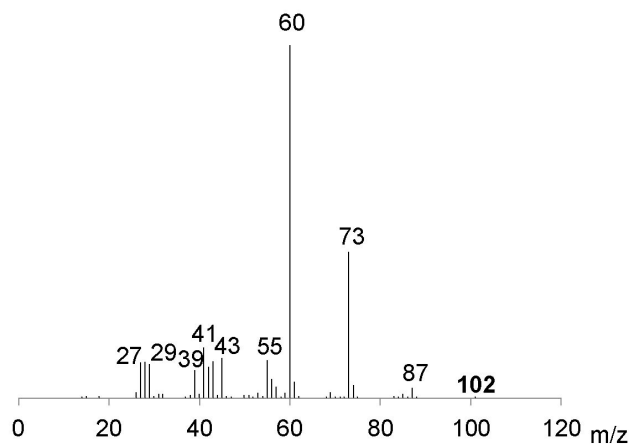
p 3-butylidihydro-2(3H)-furanone



q methyl 2-ethylhexanoate



r pentyl 2-ethylhexanoic acid



*Listed masses refer to signature fragments of the identified species, as recorded in the Agilent NIST05a library. Masses in bold represent the parent ion.

Supplemental references

- 1 A. P. Grosvenor, B. A. Kobe, M. C. Biesinger and N. S. McIntyre, *Surf. Interface Anal.*, 2004, **36**, 1564–1574.